



# Spatiotemporal variations in the hydrochemical characteristics and controlling factors of streamflow and groundwater in the Wei River of China<sup>☆</sup>

Zhou Li<sup>a</sup>, Jun Xiao<sup>b</sup>, Jaivime Evaristo<sup>a, c</sup>, Zhi Li<sup>a, \*</sup>

<sup>a</sup> State Key Laboratory of Soil Erosion and Dryland Farming on the Loess Plateau, College of Natural Resources and Environment, Northwest A&F University, Yangling, Shaanxi, 712100, China

<sup>b</sup> State Key Laboratory of Loess and Quaternary Geology, Institute of Earth Environment, Chinese Academy of Sciences, Xi'an, Shaanxi, 710061, China

<sup>c</sup> Copernicus Institute of Sustainable Development, Utrecht University, Utrecht, the Netherlands

## ARTICLE INFO

### Article history:

Received 31 March 2019

Received in revised form

16 July 2019

Accepted 1 August 2019

Available online 5 August 2019

### Keywords:

Water quality

Controlling factors

Mass balance method

Forward model

Stable isotope

## ABSTRACT

Analysis of hydrochemical characteristics and controlling factors of streamflow and groundwater in arid regions is important for water security. In this study, we collected samples of streamflow and groundwater from the Wei River in China, analyzed their hydrochemical characteristics, and identified the major solute sources using ion concentrations,  $\delta^{15}\text{N}-\text{NO}_3^-$  and  $\delta^{18}\text{O}-\text{NO}_3^-$ . The major downstream ion contents were greater than the corresponding upstream values and the ion content in streamflow during the wet season is much higher than that during the dry season. The water quality during the wet season was unsatisfactory as approximately one third of the water samples were categorized as the worst water quality based on excessive nitrates and carbonate weathering. Rock weathering contributed the greatest proportion of solutes to both streamflow and groundwater. Evaporite dissolution and carbonate weathering dominated solutes in the wet and dry seasons, respectively. Human activities cannot be ignored in certain areas. Fertilizer application accounts for 43% of the total anthropogenic solute inputs. These results point to the increasing impact of agriculture on water quality.

© 2019 Elsevier Ltd. All rights reserved.

## 1. Introduction

Surface water in human-impacted ecosystems receive solutes (i.e. nutrients and pollutants) from both point and non-point sources, affecting water quality and altering ecosystem structure and function at various space and time scales (Azzellino et al., 2008). Rivers are critical surface water resources that supply public water to cities and sustain the ecological health of constituent riparian and aquatic communities (Biol, 2008). Over the past few decades, increasing human activities, including upstream water diversion, resort and recreational activities, urban and agricultural runoff, legacy mining effects, and treated wastewater discharge, have led to increasing pressure on river water quality and a greater need for management intervention (UNEP, 2016; Wen et al., 2015). A critical first step towards the sustainable management of river water quality is problem identification through river monitoring

programs. While most river monitoring programs measure chemical concentrations (e.g., nitrate, sulfate) to quantify nutrient or solute loads that may impact water quality (Gibbs, 1970; Mateo-Sagasta et al., 2018), some programs use environmental isotopes (e.g.,  $\delta^{15}\text{N}$ -nitrate,  $\delta^{18}\text{O}$ -nitrate) to identify their sources in a given area.

The sources of solutes in rivers may be natural or anthropogenic (Grosbois et al., 2001; Meybeck, 1998; Roy et al., 1999; Xiao et al., 2016). Natural sources may include atmospheric inputs and the chemical weathering of silicates, carbonates and evaporites, while anthropogenic sources may stem from human activities in the agricultural, industrial, and domestic sectors (Flintrop et al., 1996; Han et al., 2010; Li et al., 2014). The identification of such sources can be performed using a wide range of qualitative and quantitative methods. Qualitative, methods, such as Piper diagrams (Piper, 1944), Gibbs plots (Gibbs, 1970), and factor analysis, may be used to assess water chemistry and rock weathering, respectively, for putative sources. Quantitatively, chemical concentrations or environmental isotopes may be considered in a system of mass balance equations to quantify the contributions of different sources. Forward modeling using chemical concentrations can isolate the

<sup>☆</sup> This paper has been recommended for acceptance by Dr. Jörg Rinklebe.

\* Corresponding author.

E-mail address: [lizhibox@nwfau.edu.cn](mailto:lizhibox@nwfau.edu.cn) (Z. Li).

contribution of each source of the dissolved solutes, which is helpful for the assessment of overall water chemistry (Ollivier et al., 2010; Stallard and Edmond, 1987). Source analysis based on environmental isotopes considers the proximity of isotopic values between dissolved solutes and putative sources (Cortecci et al., 2002; Phillips and Gregg, 2003). Environmental isotopes are more useful than simple chemical concentration monitoring because isotopic ratios can change even when chemical concentrations remain stable. The combined use of chemical concentration and isotope-based methods therefore enables the robust assessment and identification of river solute sources.

The Wei River is the largest tributary of the Yellow River in China (Fig. 1). Rapid industrialization since the 1980s has resulted in progressively declining river water quality, which fell to its lowest record level in 2004. Since 2008, the Chinese government has invested 2.13 billion US dollars per year for comprehensive management of the Wei River. As a result, the water quality has rating improved between 2010 and 2014 from inferior V to inferior IV. However, because of significant reductions in streamflow and the impact of human activities in recent years, the water quality of streamflow and groundwater continue to pose environmental health concerns. Although several recent studies have analyzed the water chemistry or quality for certain transects (Lu et al., 2010; Qu et al., 2017; Wang et al., 2011; Yu et al., 2016), temporal and spatial variations in hydrochemistry and their controlling factors have rarely been addressed.

The objectives of this study were to assess the current water quality of the streamflow and groundwater of the Wei River and analyze the controlling factors of water quality. We sampled streamflow and groundwater in both the wet and dry seasons, employed qualitative and quantitative modeling for assessing and identifying solute sources, and identified the processes and mechanisms controlling water quality. Our findings will inform current and future water quality management programs for the Wei River and other similar areas.

## 2. Materials and methods

### 2.1. Study area

The Wei River (Fig. 1) extends 818 km from west to east, an area of 134,766 km<sup>2</sup>. Based on a continental monsoon climate, the mean annual precipitation and potential evapotranspiration are 501.9 and 1015.0 mm, respectively (Ning et al., 2017). Low annual precipitation and high potential evapotranspiration lead to severe water shortages. The Guanzhong Plain within the Wei River catchment is a densely populated area (480 people/km<sup>2</sup>) and an important industrial and agricultural production base with a total irrigated area of 920,000 ha. The high population density and rapid economic development in this area require large amounts of water. These societal pressures result in high utilization of streamflow and groundwater, which may increase water pollution.

The north-bank tributaries originating from the Loess Plateau have loess deposits up to 350 m deep and are long with high streamflow sediment concentrations. In contrast, the south-bank tributaries originating from the Qinling Mountains have clear and rapid water flows (Sun, 2014). The elevation of the catchment decreases from west to east, ranging from 336 to 3,929 m. The aquifer is largely composed of feldspar, aluminosilicates, and carbonate (calcite, dolomite) minerals. The relative proportions are 34.8–40% for quartz, 5–20% for feldspar, 11.7–15% for calcite, and 10–15% for clay minerals. The landforms include mountainous areas, loess hills, loess tablelands, and alluvial valley plains. The landscape is dominated by farmland, grassland, and forestland, which account for 47%, 31%, and 21% of the total area, respectively (Yu et al., 2016).

### 2.2. Sample collection and analysis

To analyze spatiotemporal variations in the hydrochemistry of streamflow and groundwater, we collected water samples during the dry season (April 2013) and wet season (August 2017) from

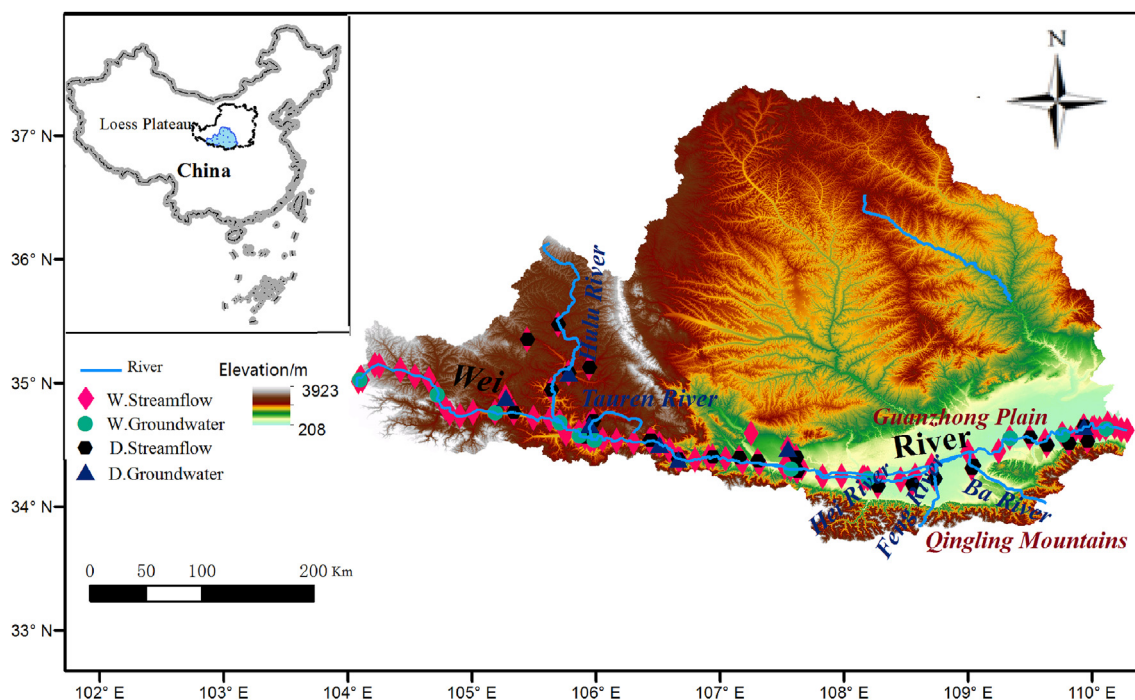


Fig. 1. Location of the Wei River and sampling sites. Streamflow and groundwater were collected for the mainstream in both dry (D.Groundwater and D. Streamflow) and wet season (W.Groundwater and W. Streamflow).

various point along the entire Wei River (total length of 818 km). We collected 27 streamflow samples and seven groundwater samples during the dry season, and collected 70 streamflow samples and 11 groundwater samples during the wet season (Fig. 1). The streamflow samples were collected using pre-washed plastic bottles and the groundwater samples were collected from wells that are 10–30 m deep after pumping each well to evacuate three times the volume of standing water in the pipe. After the water samples were collected, they were filtered in situ through 0.45- $\mu\text{m}$  Whatman® nylon filters to remove any insoluble particles. A 60-mL aliquot was stored in a pre-cleaned high-density polyethylene bottle and acidified to a pH level less than two using 6-M ultrapure  $\text{HNO}_3$  for cation analysis. A 30-mL aliquot of acidified water was collected for anion analysis and trace-element identification. We measured pH, temperature, and total dissolved solids (TDS) in situ, sealed the collected samples in 100-ml polyethylene plastic bottles and stored them at 4 °C.  $\text{HCO}_3^-$  and  $\text{CO}_3^{2-}$  levels were measured via acid-base titration (Mitamura et al., 2003).  $\text{SO}_4^{2-}$ ,  $\text{Cl}^-$ ,  $\text{F}^-$  and  $\text{NO}_3^-$  levels were determined using ion chromatography (ICS-1100, Dionex). The major cations, namely  $\text{Na}^+$ ,  $\text{Mg}^{2+}$ ,  $\text{K}^+$ ,  $\text{Ca}^{2+}$ ,  $\text{Fe}$ ,  $\text{As}$ ,  $\text{Cr}$ ,  $\text{Cd}$ , and  $\text{Cu}$ , were analyzed using a total Spectral Plasma Spectrometer (ICP-MS, Thermos Fisher Scientific) at the Water Environment Research Lab of Northwest A&F University. The stable nitrogen and oxygen isotopes in the nitrates ( $\delta^{15}\text{N}-\text{NO}_3^-$  and  $\delta^{18}\text{O}-\text{NO}_3^-$ ) were analyzed at the Third Institute of Oceanography of the State Oceanic Administration following the denitrifying bacterial method using stable isotope mass spectrometer (Gas-Bench-Mat253, Thermos Fisher Scientific). The water samples were pre-processed by converting  $\text{NO}_3^-$  into gaseous  $\text{N}_2\text{O}$  for detection using a continuous-flow isotope ratio mass spectrometer (IRMS, Isoprime100). In this paper, isotope ratio values are reported in parts per thousand (‰) relative to  $\text{N}_2$  (air) and Standard Mean Ocean Water for  $\delta^{15}\text{N}-\text{NO}_3^-$  and  $\delta^{18}\text{O}-\text{NO}_3^-$ . The analytical precisions levels for  $\delta^{15}\text{N}-\text{NO}_3^-$  and  $\delta^{18}\text{O}-\text{NO}_3^-$  are  $\pm 0.2\text{‰}$  and  $\pm 0.3\text{‰}$ , respectively.

### 2.3. Interpreting the controlling factors of hydrochemistry

To compare the ionic compositions of streamflow and groundwater, we plotted the data in a Piper diagram. We then classified water quality using fuzzy membership functions according to the *Environmental Quality Standard for Surface Water and Groundwater in China* (Tables S1 and S2), based on the method described by Zhang et al. (2012).

Next, qualitative analysis was performed to identify major controlling factors, and quantitative analysis was performed to break down the contributions of various factors to the dissolved solutes. For qualitative analysis, a Gibbs plot and factor analysis was employed to identify the major controlling factors of streamflow and groundwater hydrochemistry. Specifically, a Gibbs plot was employed to investigate the contributions of different sources, such as atmospheric inputs, human activities, and rock weathering, to hydrochemistry by plotting TDS versus  $\text{Na}/(\text{Na} + \text{Ca})$  and TDS versus  $\text{Cl}/(\text{Cl} + \text{HCO}_3)$ . Principal component analysis (PCA) was employed to transform inter-correlated hydrochemical indicators into uncorrelated variables (Villegas et al., 2013). PCA was performed for ten indicators:  $\text{K}^+$ ,  $\text{Ca}^{2+}$ ,  $\text{Na}^+$ ,  $\text{Mg}^{2+}$ ,  $\text{Cl}^-$ ,  $\text{SO}_4^{2-}$ ,  $\text{HCO}_3^-$ ,  $\text{NO}_3^-$ ,  $\text{F}^-$ , and TDS. To identify sources of nitrate, the isotopic compositions of nitrogen and oxygen in the nitrates ( $\delta^{15}\text{N}-\text{NO}_3^-$ ,  $\delta^{18}\text{O}-\text{NO}_3^-$ ) were compared to published values.

For quantitative analysis, a forward model for mass budget calculation was adopted to calculate the contributions of atmospheric inputs, human activities, and rock weathering (e.g., carbonate, silicate, and evaporite) to the dissolved solutes. The mass budget equation for any element X is defined as follows:

$$X_{\text{water}} = X_{\text{atm}} + X_{\text{eva}} + X_{\text{sil}} + X_{\text{carb}} + X_{\text{anth}}, \quad (1)$$

where water represents surface water or groundwater and atm, anth, sil, carb and eva refer to atmospheric input, anthropogenic input, silicate weathering, carbonate weathering, and evaporite dissolution, respectively. To calculate each component on the right side of Equation (1), additional pertinent data and equations are required as detailed in Section 3.2.

The mass balance of stable isotope was used to calculate the contribution of each source to the nitrates in water as follows:

$$\delta^{15}\text{N} = \sum_{i=1}^n f_i \times \delta^{15}\text{N}_i, \quad (2)$$

$$\delta^{18}\text{O} = \sum_{i=1}^n f_i \times \delta^{18}\text{O}_i, \quad (3)$$

$$1 = \sum_{i=1}^n f_i, \quad (4)$$

where  $i$  refers to the number of nitrate sources and  $f_i$  refers to the fraction of a specific nitrate source.

To interpret the potential impacts of surface water-groundwater flow paths on solutes, we analyzed the surface water-groundwater relationship using the chloride mass balance method as follows:

$$Q_s \cdot C_s = Q_u \cdot C_u + (Q_s - Q_u) \cdot C_v, \quad (5)$$

where  $Q_s$  is the total water flux;  $Q_u$  and  $Q_s - Q_u$  are the fluxes of the two endmembers; and  $C_s$ ,  $C_u$ , and  $C_v$  are the chloride concentrations in different types of water.

## 3. Results

### 3.1. pH and total dissolved solids

Table S3 lists the pH, TDS, and ion concentrations of streamflow and groundwater. The pH values range from 7.26 to 9.27 with a mean of 8.10. The TDS range from 194.3 to 2136.8 M with a mean of 666.4 M, indicating slight alkalinity and high salinity. Furthermore, these values vary with the seasons and are noticeably different for streamflow and groundwater. In the wet season, the pH values (mean  $\pm 1$  SD) of streamflow and groundwater are  $8.16 \pm 0.31$  and  $7.63 \pm 0.21$ , respectively, and the TDS values were  $551.9 \pm 283.2$  and  $812.1 \pm 405.7$  M, respectively. During the dry season, the pH values of streamflow and groundwater are  $8.38 \pm 0.36$  and  $7.87 \pm 0.27$ , respectively, and the TDS values are  $667.6 \pm 337.8$  and  $748.2 \pm 581.7$  M, respectively.

### 3.2. Hydrochemical composition and water type

The concentrations of major cations in the streamflow and groundwater were similar between the two seasons in the order of  $\text{Ca}^{2+} > \text{Na}^+ > \text{Mg}^{2+} > \text{K}^+$ , while the anions were in the order of  $\text{HCO}_3^- > \text{SO}_4^{2-} > \text{NO}_3^- > \text{Cl}^-$ . During the dry and wet season, the dominant cation was  $\text{Ca}^{2+}$ , accounting for  $38 \pm 10\%$  to  $86 \pm 19\%$  of the  $\text{TZ}^+$  ( $\text{TZ}^+ = \text{Na}^+ + \text{K}^+ + 2\text{Mg}^{2+} + 2\text{Ca}^{2+}$ ), while the dominant anion was  $\text{HCO}_3^-$ , accounting for  $37 \pm 6\%$  to  $61 \pm 20\%$  of the  $\text{TZ}^-$  ( $\text{TZ}^- = \text{NO}_3^- + \text{F}^- + \text{Cl}^- + 2\text{SO}_4^{2-} + \text{HCO}_3^-$ ). The water chemistry type changed from Ca–Mg– $\text{HCO}_3$  in the dry season to Ca–Mg– $\text{SO}_4$ –Cl in the wet season (Fig. 2). Additionally, the streamflow and groundwater data overlapped, possibly which may be a result of



### Broad classification of water types

- 1-Ca-Mg-HCO<sub>3</sub>
- 2-Na-Cl-SO<sub>4</sub>
- 3-Na-HCO<sub>3</sub>
- 4-Ca-Mg-SO<sub>4</sub>-Cl

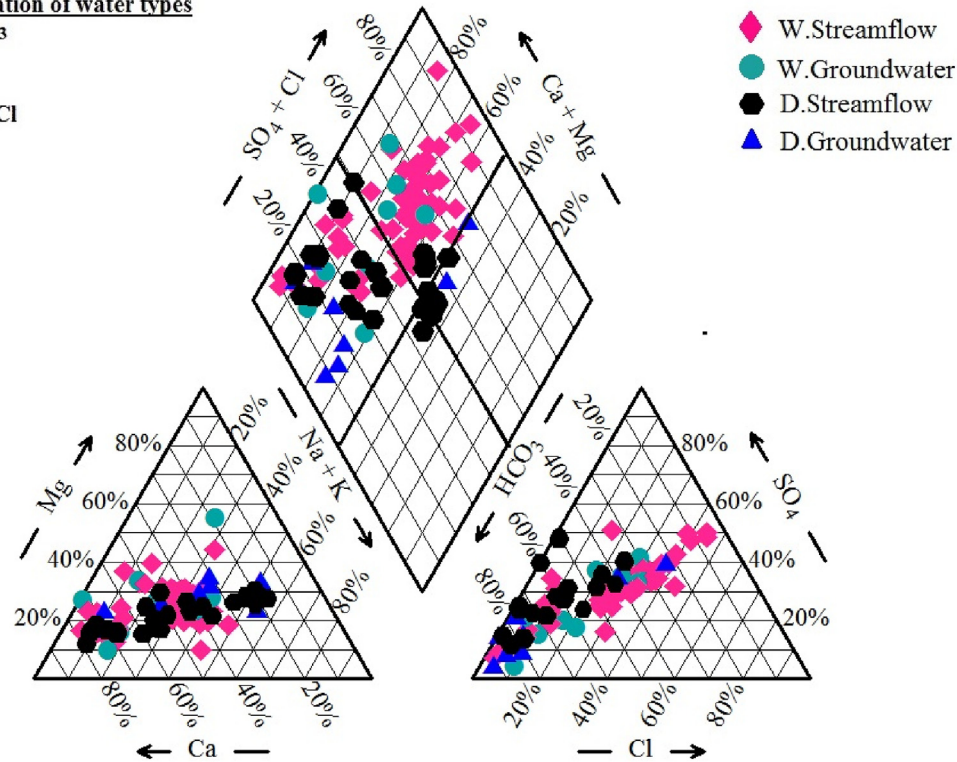


Fig. 2. Piper diagram of chemical compositions for streamflow and groundwater.

streamflow-groundwater interactions.

### 3.3. Spatiotemporal variations in water chemistry and quality

To explore the spatial patterns of hydrochemistry, the major ions of streamflow concentrations were plotted against longitude to illustrate the eastward flow of the Wei River (Fig. 3). During the wet season, the concentrations of major ions in the middle and lower reaches are greater than those in the upper reach. The upstream concentrations changes lightly from the dry season to the wet season compared to the middle and lower reaches. However, the spatial variability in the dry season was smaller than in the wet season. In particular, the concentration of NO<sub>3</sub><sup>-</sup> in streamflow during the wet season is significantly higher than that in the dry season (standard deviations of 95.63 and 2.32, respectively) (Table S3). This indicates that streamflow in the dry season is less affected by human activities.

Regarding temporal streamflow, 29% of the samples belong to class V in the wet season, but 97% of the samples belong to classes I–III in the dry season (classes I, II, and III accounted for 30%, 37%, and 30% of the total samples, respectively). For groundwater, 36% of the samples belong to class V in the wet season. The samples in the dry season for class I, II and V accounted for 25%, 50%, and 25%, respectively (Table 3). It appears that the wet season has worse overall water quality compared to the dry season because more water samples belong to class V for the wet season. Spatially, we calculated the percentages of different classes among the total number of water samples for both the dry and wet seasons. For streamflow, the upstream samples of classes I–III, IV, and V account for 24%, 0%, and 3% of the total number of streamflow samples, respectively, and the corresponding values are 24%, 1%, and 18%, respectively, for the middle reach, and 28%, 1%, and 0%, respectively, for the lower reach. For groundwater, the upstream samples of

classes I–III and V account for 38% and 12% of the total number of groundwater samples, and the corresponding values were 13% and 5%, respectively, for the middle reach, and 22% and 10%, respectively, for the lower reach.

## 4. Discussion

### 4.1. Controlling factors for dissolved solutes

To identify the dominant process controlling dissolved solutes, Gibbs diagram and Na-normalized molar ratios were employed (Gaillardet et al., 1999). Most water samples had low Na/(Na + Ca) and Cl/(Cl + HCO<sub>3</sub><sup>-</sup>) levels, but moderate TDS, indicating typical rock-dominated waters solutes (Fig. 4a and b).

To clarify the major lithologies contributing to dissolved solutes, the Na-normalized molar ratios method was adopted. This method divides the main sources of ions into evaporite dissolution, silicate rocks, and carbonate rocks. The elemental ratio adjusted by Na<sup>+</sup> can effectively eliminate dilution effects (Gaillardet et al., 1995; Gaillardet et al., 1999). The wet-season samples were affected by all the three types of rock salts. In contrast, most dry-season groundwater samples fell in the upper right section (Fig. 4c and d), indicating that the dissolved solutes are largely affected by carbonate weathering.

### 4.2. Contributions of different sources to dissolved solutes

The contributions of different factors, namely atmospheric inputs, human activities, and rock weathering, to the dissolved solutes were quantified using a forward model (Fig. S1). Overall, silicate weathering accounts for 33 ± 4% of streamflow and groundwater solutes, with no detectable seasonal differences. Carbonate weathering and evaporite dissolution exhibit significant

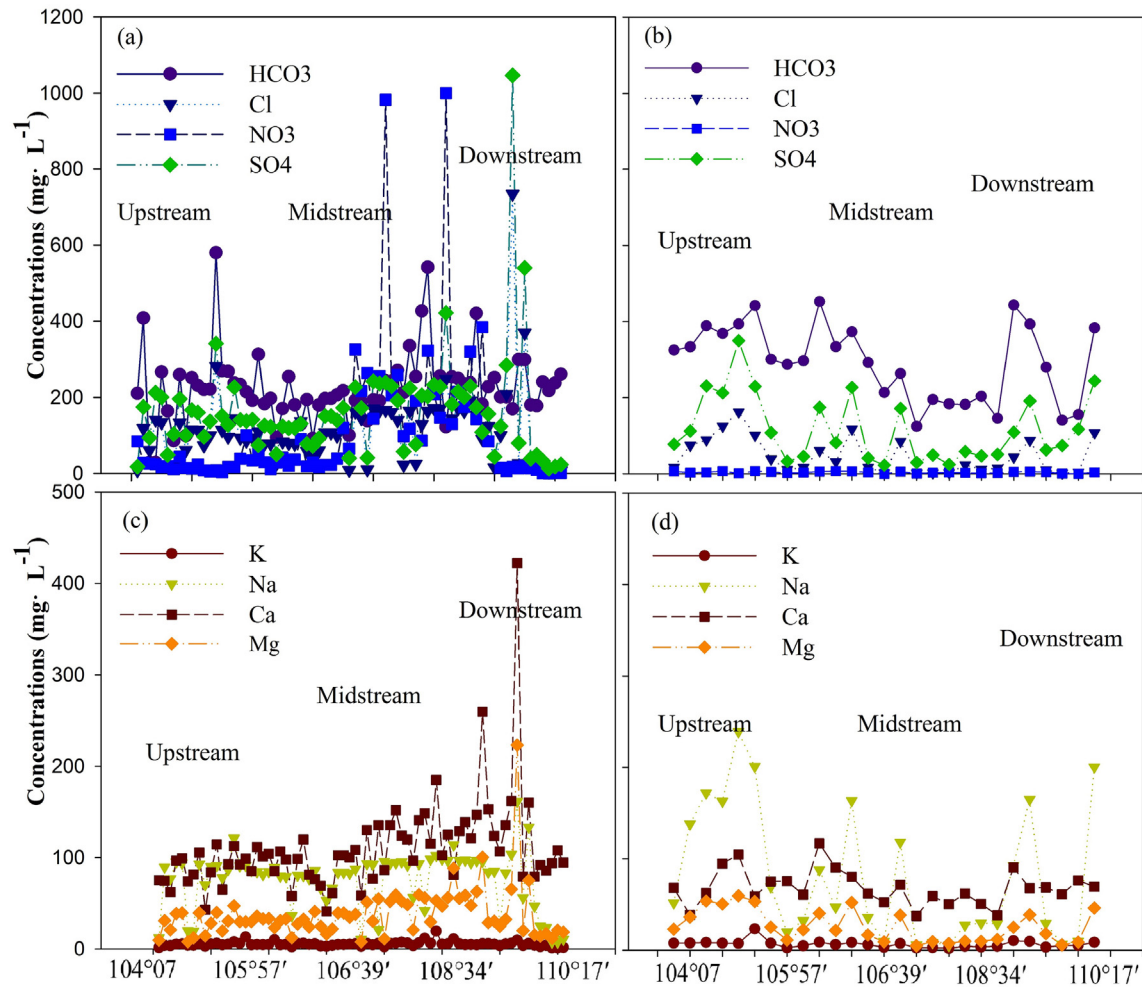


**Fig. 3.** Spatiotemporal variations in streamflow hydrochemistry in wet and dry season. Major anion contents in wet season (a) and dry season (b), major cation contents in wet season (c) and dry season (d).

seasonal changes, with the former accounting for  $51 \pm 21\%$  of groundwater solutes, with a strong seasonal signal during the dry season. The latter accounts for  $46 \pm 5\%$  of groundwater solutes with a stronger seasonal signal during the wet season. Human activities account for  $10 \pm 5\%$  of dissolved solutes in streamflow. The effects of atmospheric inputs and human activities for other water types and seasons are negligible.

**4.2.1. Atmospheric inputs**

The contributions of atmospheric inputs were largely calculated from rainfall chemical compositions. In practice,  $Cl^-$  is commonly used to calculate the proportion of dissolved solutes derived from the atmosphere because it is stable and conservative (Moon et al., 2007). To estimate the contributions of atmospheric inputs, all samples with low  $Cl^-$  levels are assumed to obtain  $Cl^-$  from the atmosphere (Hyonjeong et al., 2009; Rai et al., 2010). When the lowest  $Cl^-$  level ( $Cl^-_{min}$ ) in the sample is greater than the rainwater  $Cl^-$  concentration, the total amount of atmospheric input can be calculated and corrected using the following formulas:

$$X_{rain}^* = X_{rain} \times Cl^-_{min} / Cl^-_{rain}, \tag{6}$$

$$X_{rw}^* = X_{rw} - X_{rain}^*, \tag{7}$$

where  $X_{rain}$  is the concentration of X in rain and  $X_{rain}^*$  represents the corrected concentration.  $X_{rw}$  is the concentration of X in streamflow or groundwater and  $X_{rw}^*$  represents the corrected concentration.

Precipitation chloride data was obtained from the East Asia Acid Rain Network. The contributions of atmospheric inputs account for  $8 \pm 3\%$  of streamflow in the dry season and  $5 \pm 3\%$  of streamflow in the wet season. Despite slight seasonal variations, the effects of atmospheric inputs on streamflow and groundwater are low overall, which is intuitive based on the fact that the Wei River is located far from the ocean.

**4.2.2. Human activities**

Human activities always contribute to variations in water chemistry and quality. The Guanzhong Plain is an important agricultural and industrial production base and the most densely populated area in the catchment. According to the National Bureau of Statistics of China, 26.7 million tons of fertilizer (converted to pure nitrogen) were applied in the research area from 2004 to 2013 with utilization rates of 30–40% for nitrogen fertilizer, 10–25% for phosphate fertilizer, and 40–60% for potassium fertilizer. These activities inevitably affect the water quality in the Wei River. The pollutants from human activities are typically characterized as being rich in  $K^+$ ,  $Ca^{2+}$ ,  $SO_4^{2-}$ ,  $Cl^-$ , and  $NO_3^-$  (Redwan and Abdel Moneim, 2016); however,  $K^+$ ,  $Ca^{2+}$ ,  $SO_4^{2-}$ ,  $Cl^-$  are also products of

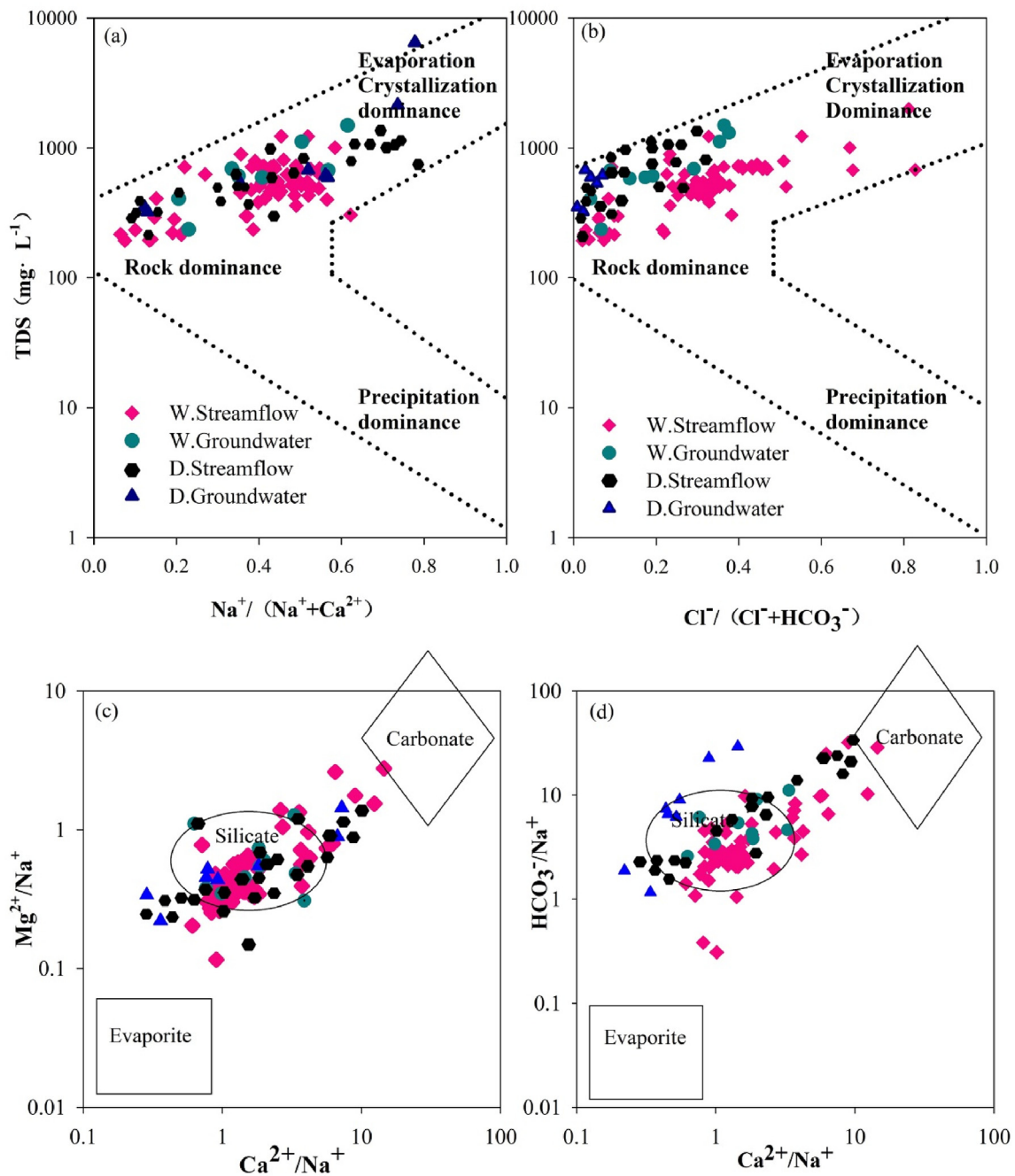


**Fig. 4.** Gibbs diagram of streamflow and groundwater hydrochemistry for (a) cation ratios and (b) anion ratios. (c) Mg/Na versus Ca/Na and (d) HCO<sub>3</sub>/Na versus Ca/Na for streamflow and groundwater.

rock weathering. Therefore, NO<sub>3</sub><sup>-</sup> was considered as an indicator of human activities in this study.

According to the PCA results (Table 1), the scores of K<sup>+</sup> and NO<sub>3</sub><sup>-</sup> are very similar for factor 2 of streamflow during the wet season, representing the influence of excessive application of nitrogen and potassium fertilizers. Because chloride concentrations are typically stable in nature, but can be increased by human activities, we compared the concentrations of Cl<sup>-</sup> to those of NO<sub>3</sub><sup>-</sup> to identify nitrate sources qualitatively (Fig. 5a). The concentrations of both Cl<sup>-</sup> and NO<sub>3</sub><sup>-</sup> in the headwater region are low, indicating that they are not influenced by intensive human activities. However, as the river flows through farming and urban areas, the concentrations of

Cl<sup>-</sup> and NO<sub>3</sub><sup>-</sup> increase based on the application of fertilizer (high NO<sub>3</sub><sup>-</sup> and low Cl<sup>-</sup>) and manure (high NO<sub>3</sub><sup>-</sup> and high Cl<sup>-</sup>). Additionally, dual-isotope comparisons between nitrogen and oxygen in various wet-season samples indicated that fertilizers, soil nitrogen, manure, and sewage are potential main nitrate sources, but the former two sources likely contribute relatively large amounts of nitrate (Fig. 5b).

Because nitrates represent human activities, we quantified the contributions of anthropogenic inputs to nitrate in streamflow and groundwater in different seasons using a forward model. Anthropogenic inputs make the greatest contribution to streamflow nitrates during the wet season with an average contribution of

**Table 1**  
Varimax loading of the variables for each factor in wet and dry season.

	Variable	Streamflow			Groundwater		
		Factor 1	Factor 2	Factor 3	Factor 1	Factor 2	Factor 3
Dry season	SO <sub>4</sub> <sup>2-</sup>	<b>0.93</b>	0.3	-0.02	0.71	<b>0.69</b>	0.11
	Cl <sup>-</sup>	<b>0.88</b>	0.38	-0.05	0.76	<b>0.64</b>	0.07
	Mg <sup>2+</sup>	<b>0.83</b>	0.52	-0.03	0.23	<b>0.91</b>	<b>0.28</b>
	TDS	<b>0.86</b>	0.48	0.09	<b>0.85</b>	<b>0.53</b>	0.04
	Ca <sup>2+</sup>	<b>0.53</b>	0.16	<b>0.65</b>	<b>0.82</b>	<b>0.57</b>	0.05
	Na <sup>+</sup>	<b>0.87</b>	0.44	-0.11	<b>0.88</b>	<i>0.46</i>	-0.07
	HCO <sub>3</sub> <sup>-</sup>	-0.15	0.02	<b>0.88</b>	<b>0.95</b>	0.24	-0.06
	K <sup>+</sup>	0.45	<b>0.72</b>	-0.15	0.69	<b>0.68</b>	<b>0.22</b>
	F <sup>-</sup>	<b>0.78</b>	0.09	0.21	-0.01	-0.2	-0.97
	NO <sub>3</sub> <sup>-</sup>	0.15	<b>0.89</b>	0.29	0.86	0.09	<b>0.46</b>
	Eigenvalue	4.95	2.26	1.37	5.4	3.09	1.3
	%Total variance	49.53	22.56	13.67	54.04	30.94	13
	Cumulative % variance	49.53	72.09	<b>85.76</b>	54.04	84.98	<b>97.98</b>
	Wet season	SO <sub>4</sub> <sup>2-</sup>	<b>0.96</b>	0.10	0.15	<b>0.96</b>	0.06
Cl <sup>-</sup>		<b>0.96</b>	0.17	0.14	<b>0.96</b>	-0.01	0.03
Mg <sup>2+</sup>		<b>0.95</b>	0.11	-0.1	<b>0.83</b>	0.22	-0.47
TDS		<b>0.89</b>	0.30	0.21	<b>0.93</b>	0.27	-0.11
Ca <sup>2+</sup>		<b>0.84</b>	0.15	-0.26	<b>0.67</b>	-0.58	-0.09
Na <sup>+</sup>		0.71	0.45	0.21	<b>0.83</b>	0.3	-0.16
HCO <sub>3</sub> <sup>-</sup>		0.07	<b>0.83</b>	0	0.44	0.44	<b>0.62</b>
K <sup>+</sup>		0.37	<b>0.69</b>	0.09	0.63	-0.37	<b>0.39</b>
F <sup>-</sup>		0.15	0.16	<b>0.89</b>	-0.01	<b>0.9</b>	0.2
NO <sub>3</sub> <sup>-</sup>		0.1	<b>0.47</b>	-0.52	0.66	-0.35	<b>0.47</b>
Eigenvalue		5.53	1.27	1.16	5.47	1.82	1.07
%Total variance		49.17	17.75	12.7	42.08	26.05	15.48
Cumulative % variance		49.17	66.92	79.6	42.08	68.13	83.61

Bold and italic values indicate strong and moderate loadings, respectively.

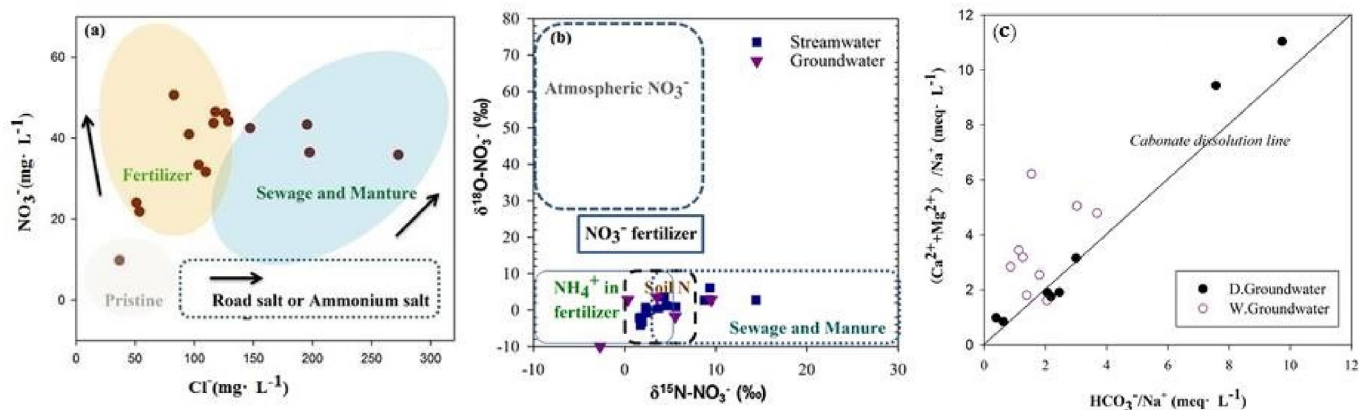


**Fig. 5.** (a) Mixing diagram of NO<sub>3</sub><sup>-</sup> and Cl<sup>-</sup> concentrations for streamflow in the wet season. (b) Dual isotope comparison for δ<sup>15</sup>N-NO<sub>3</sub><sup>-</sup> and δ<sup>18</sup>O-NO<sub>3</sub><sup>-</sup> for streamflow in the wet season. Boxes represent ranges in isotopic signatures of N and O for different nitrate sources. (c) Stoichiometry plots of groundwater in dry and wet season.

10 ± 5%. Their contributions to streamflow and groundwater nitrates during the dry season are relatively small (Fig. S1). Furthermore, we quantified the contributions of different human activities to nitrate concentrations based on the mass balance of nitrate isotopes and found that the mean contribution was the highest for chemical fertilizer (42.7%), intermediate for soil nitrogen (31.2%), and smallest for sewage and manure (26.1%) (Table 2). The nitrate content in streamflow and groundwater during the wet season is over 20 times greater than that in dry season. It seems that the nitrate in water bodies is washed out of soil by surface runoff, meaning the nitrate in streamflow and groundwater may be dominated by agricultural activities. Nitrogen and oxygen stable isotopes support this hypothesis. Specifically, dual-isotope comparisons of nitrogen and oxygen in various wet-season samples indicated that fertilizers, soil nitrogen, manure, and sewage are plausible main nitrate sources, but the former two sources likely

contributed the majority of nitrates (Fig. 5b). Therefore, it can be concluded that the nitrate in streamflow and groundwater stems from agricultural activities, but flows into the Yellow River to increase water pollution in the middle and lower reaches of the river.

#### 4.2.3. Rock weathering

PCA revealed that factor 1 of streamflow and groundwater for the wet season is highly correlated with Ca<sup>2+</sup>, Na<sup>+</sup>, Mg<sup>2+</sup>, Cl<sup>-</sup>, SO<sub>4</sub><sup>2-</sup>, and TDS (Table 1) with contributions to the total variance of 49 ± 28% and 42 ± 18%, respectively. This indicates a major contribution from evaporite dissolution during the wet season. In general, halite (Na<sup>+</sup>: Cl<sup>-</sup> = 1:1) and gypsum (CaSO<sub>4</sub>·2H<sub>2</sub>O) or anhydrite are the main sources of SO<sub>4</sub><sup>2-</sup> and Cl<sup>-</sup>. In addition to atmospheric precipitation input, Cl<sup>-</sup> in streamflow and groundwater is also derived from rock weathering. In addition to the hydrolysis of gypsum, SO<sub>4</sub><sup>2-</sup> may also be derived from the oxidation of



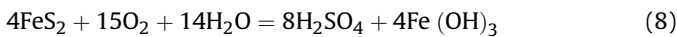
**Table 2**  
Proportional contributions of three potential nitrate sources to streamflow and groundwater in the Wei River during the wet season.

Category	Site	Chemical Fertilizer (%)	Soil organic N (%)	Sewage and Manure (%)
Streamflow	S1	45 ± 1.4	31 ± 1.4	24 ± 0
	S2	35 ± 1.2	40 ± 1.2	25 ± 1.2
	S3	65 ± 1.6	9 ± 5.8	26 ± 15.6
	S4	26 ± 1.6	49 ± 1.2	25 ± 1.6
	S5	21 ± 2	23 ± 3.2	56 ± 2.8
	S6	48 ± 1.6	42 ± 1.6	10 ± 1.6
	S7	24 ± 1.2	39 ± 1.2	37 ± 1.2
	S8	73 ± 1.6	2 ± 1.9	25 ± 1.0
	S9	70 ± 8.5	10 ± 6.1	20 ± 7.8
	S10	20 ± 1.2	67 ± 1.2	13 ± 1.2
	Average	42.7	31.2	26.1
Groundwater	G1	46 ± 4.0	44 ± 10.0	10 ± 6.0
	G2	14 ± 7.4	28 ± 2.8	58 ± 7.5
	G3	21 ± 15.0	48 ± 25.2	31 ± 10.2
	G4	90 ± 1.7	6 ± 2.1	4 ± 2.1
	G5	13 ± 11.7	27 ± 18.1	59 ± 6.4
		Average	36.8	30.6

**Table 3**  
Water quality classification by the fuzzy membership function.

Water samples		Number of samples within class					Total
		I	II	III	IV	V	
Streamflow	Wet season	17	25	6	2	20	70
	Dry season	8	10	8	0	1	27
Groundwater	Wet season	2	4	1	0	4	11
	Dry season	2	4	0	0	1	7
Total		29	43	15	2	26	115

pyrite as follows:



However, there is no pyrite and little sulfuric acid in the precipitation in the Yellow River basin (Larssen et al., 1999). Therefore, only rock salt and gypsum dissolution were considered in this study when calculating evaporite dissolution as follows:

$$\text{Cl}_e = \text{Cl}_{\text{river}} - \text{Cl}_{\text{rain}}, \quad \text{Na}_e = \text{Cl}_e, \quad \text{Halite\%} = \text{Cl}_e / \text{llitela}_{\text{total}}, \quad (9)$$

$$\text{SO}_{4e} = \text{SO}_{4\text{river}} - \text{SO}_{4\text{rain}}, \quad \text{Ca}_e = \text{SO}_{4e}, \quad \text{Gypsum\%} = \text{SO}_{4e} / \text{eypsuma}_{\text{total}}, \quad (10)$$

where  $\text{Cl}_{\text{river}}$  and  $\text{Cl}_{\text{rain}}$  are the concentration of Cl in the river and rain, respectively.  $\text{Cl}_e$  represents the Cl in river water after correction for rain inputs. Halite% is the contribution rate of halite dissolution to the solute in evaporite.  $\text{SO}_{4\text{river}}$  and  $\text{SO}_{4\text{rain}}$  are the concentrations of  $\text{SO}_4$  in the river and rain, respectively.  $\text{SO}_{4e}$  represents the  $\text{SO}_4$  in river water after correction for rain inputs. Gypsum% is the contribution rate of gypsum dissolution to solute in the evaporite.

The contributions of evaporite dissolution are  $42 \pm 18\%$  and  $49 \pm 28\%$  for wet-season streamflow and groundwater, respectively, and  $32 \pm 15\%$  and  $9 \pm 2\%$  for dry-season streamflow and groundwater, respectively. Evaporite dissolution contributes more to dissolved solutes during the wet season compared to the dry season. The evaporite dissolution rate was estimated to be 40 to 80 times greater than that of granite and 4 to 7 times greater than that of carbonate. Despite the low overall content, evaporite dissolution has a significant effect on the chemical composition of waters (Xiao et al., 2016). High temperature and rainfall during the wet season in the study area accelerate evaporite dissolution.

The concentration of silicon in the middle reaches of the Yellow River is 282–347  $\mu\text{M}$  (Fan et al., 2014). Additionally, the aquifer medium of the groundwater system contains many minerals, including feldspar, alum inosilicates, and carbonate (calcite, dolomite) minerals. Therefore, streamflow and groundwater may be affected by the weathering of silicates and carbonates. Based on our forward model, silicate weathering exhibits no significant seasonal differences, but it contributes to streamflow and groundwater solutes with an average contribution of  $33 \pm 4\%$ .

Stoichiometric approaches are often used to trace the source of groundwater solutes qualitatively (Han et al., 2010). Under natural conditions, the  $(\text{Ca} + \text{Mg})/\text{HCO}_3$  equivalent ratio from carbonate weathering is equal to one. According to Fig. 5c, the ratio of  $(\text{Ca} + \text{Mg})/\text{HCO}_3$  equivalent for most dry-season water samples is close to one, whereas the ratio of wet-season groundwater samples is greater than one, indicating that the  $\text{Ca}^{2+}$  and  $\text{Mg}^{2+}$  in dry-season groundwater are largely affected by carbonic acid (Sarin et al., 1992). Additionally, factor 1 in the factor analysis exhibits high loadings of TDS,  $\text{Ca}^{2+}$ ,  $\text{Na}^+$ , and  $\text{HCO}_3^-$  during the dry season, accounting for 54% to the total variance (Table 1). The forward model reveals that groundwater during the dry season is dominated by carbonate weathering, but it is largely affected by evaporite dissolution during the wet season. The contributions of carbonates weathering were respectively  $51 \pm 21\%$  and  $8 \pm 6\%$  for the dry and wet season. Leaching experiments on carbonate weathering conducted under different climatic conditions have shown that the weathering of carbonates is more pronounced under dry and cold conditions. In a continental monsoon climate, the dry season has low temperatures and the wet season has high temperatures. Therefore, there are seasonal variations in the dissolution of groundwater carbonates.



### 4.3. Impacts of streamflow-groundwater interactions

Streamflow-groundwater interactions have a significant impact on solute transport in water. Dry-season streamflow-groundwater relationships are dominated by one-way flow paths from groundwater to surface water, which was confirmed through in-situ observations and our previous studies using water-stable isotopes (Li et al., 2019; Li et al., 2017). Based on the chloride mass balance method, we investigated streamflow-groundwater relationships more extensively. As average values for each reach, during the dry season, groundwater recharges streamflow by 51%, 81%, and 54% for the upper, middle, and lower reaches, respectively, while the other contributions came from upstream river flow. During the wet season, the streamflow recharged groundwater by 73%, 50%, and 72% for the upper, middle and lower reaches, respectively. The flow path during the dry season runs from groundwater to streamflow, but that during the wet season is from streamflow to groundwater.

Seasonally varying streamflow-groundwater relationships can help us to interpret temporal variations in water chemistry and quality. Wet-season groundwater is dominated by streamflow, which largely stems from rainfall-derived surface runoff, which flushes the soil surface strongly and carries additional solutes. Therefore, wet-season streamflow and groundwater have higher ion concentrations and lower water quality compared to dry-season streamflow and groundwater. Spatial variations in water chemistry and quality are strongly related to river discharge. As discharge increases along the flow path from the upper reach to the lower reach, streamflow can carry more solutes into the river. As a result, the ion concentrations in the middle and lower reaches are greater and more variable than those in the upper reach.

### 4.4. Attribution of water quality

The hydroparameters responsible for water quality during the wet season are different from those during the dry season. Specifically, excessive  $\text{NO}_3^-$  causes a deterioration in the quality of streamflow with 42% of samples exceeding the water quality standard for  $\text{NO}_3^-$ . Additionally,  $\text{NO}_3^-$ ,  $\text{SO}_4^{2-}$  and TDS simultaneously result in poor groundwater quality, with 36%, 36%, and 36% of samples exceeding the water quality standards for these three ions, respectively. For streamflow, PC2 accounts for 17.75% of the variance with high loadings of  $\text{HCO}_3^-$ ,  $\text{K}^+$ , and  $\text{NO}_3^-$ . For groundwater, PC1 is dominated by  $\text{Na}^+$ ,  $\text{SO}_4^{2-}$ ,  $\text{Cl}^-$ ,  $\text{Ca}^{2+}$ ,  $\text{Mg}^{2+}$ , and TDS, accounting for 42.08% of the variance.  $\text{NO}_3^-$  has high loadings for PC3 and is responsible for 15.48% of the variance. The inter-correlated elements within each PC may stem from the same source (Table 1). For example,  $\text{NO}_3^-$  largely originates from anthropogenic activities (Sun et al., 2011). According to the National Bureau of Statistics, the application of compound fertilizers, potash fertilizers and vegetable fertilizers continuously increased during the period of 2000–2015 in the study area. Therefore, the  $\text{HCO}_3^-$ ,  $\text{K}^+$ , and  $\text{NO}_3^-$  may originate from compound fertilizers, such as  $\text{NH}_4\text{HCO}_3$  and  $\text{KNO}_3$ , whereas  $\text{SO}_4^{2-}$  and  $\text{Mg}^{2+}$  may originate from vegetable fertilizers, such as  $\text{MgSO}_4$ . Additionally,  $\text{Na}^+$  and  $\text{Cl}^-$  ions in groundwater may originate from manure application (Kim et al., 2009).

In summary, according to the results of our forward model, dissolved solutes are dominated by rock weathering, which is consistent with previous studies conducted in the study area (Xiao et al., 2016). However, regarding water quality, carbonate weathering (e.g. calcite and dolomite), manure application, and fertilizers are the major sources of groundwater pollution during the wet season, whereas impacts on streamflow quality during the wet season are dominated by fertilizers. Regarding the impacts of human activities, which were investigated based on nitrates, the contribution of fertilizer application is much greater than that of

sewage (Table 3). Agricultural activities play an important role in altering water chemistry and quality. Therefore, they should be the focus of efforts to improve water quality, especially by improving poor fertilizer utilization efficiency.

## 5. Conclusions

Regions with water shortages are often threatened by water quality degradation, which is of greater concern in arid regions. We considered the Wei River in northwest China as a study area to analyze water chemistry, quality, and solute sources in streamflow and groundwater. The major ion concentrations in the middle and lower reaches were greater than those in the upper reach, and the values during the wet season were much higher than those during the dry season. Although water quality degradation was dominated by rock weathering, dissolved solutes also originated from human activities, particularly agriculture. Although anthropogenic inputs make small contributions to solutes, they can deteriorate water quality significantly through nitrate loading, especially during the wet season. Our results suggest that pollution from non-point sources can be severe during the wet season in arid regions because of intense rainstorms and excessive fertilizer application.

## Conflicts of interest

The authors have no conflict of interest to declare.

## Acknowledgements

This study was jointly funded by the National Natural Science Foundation of China (41761144060), International Partnership Program of Chinese Academy of Sciences (161461KYSB20170013) and Natural Science Foundation of Shaanxi Province (2018JZ4001). The constructive comments from the three referees are greatly appreciated.

## Appendix A. Supplementary data

Supplementary data to this article can be found online at <https://doi.org/10.1016/j.envpol.2019.113006>.

## References

- Azzellino, A., Salvetti, R., Vismara, R., 2008. Combined Use of Watershed Models to Assess the Apportionment of Point and Non Point Load Sources to Surface Waters. Springer Netherlands, Dordrecht, pp. 369–383.
- Biról, E., 2008. Using Economic Valuation Techniques to Inform Water Resources Management in the Southern European, Mediterranean and Developing Countries: A Survey and Critical Appraisal of Available Techniques. Springer Netherlands, Dordrecht, pp. 135–155.
- Cortecchi, G., Dinelli, E., Bencini, A., Adorni-Braccesi, A., Ruffa, G.L., 2002. Natural and anthropogenic SO sources in the Arno river catchment, northern Tuscany, Italy: a chemical and isotopic reconnaissance. *Appl. Geochem.* 17, 79–92.
- Fan, B.L., Zhao, Z.Q., Tao, F.X., Liu, B.J., Tao, Z.H., Gao, S., Zhang, L.H., 2014. Characteristics of carbonate, evaporite and silicate weathering in Huanghe River basin: a comparison among the upstream, midstream and downstream. *J. Asian Earth Sci.* 96, 17–26.
- Flintrop, C., Hohlmann, B., Jasper, T., 1996. Anatomy of pollution: rivers of North Rhine-Westphalia, Germany. *Am. J. Sci.* 296, 58–98.
- Gaillardet, J., Dupré, B., Allègre, C.J., 1995. A global geochemical mass budget applied to the Congo basin rivers: erosion rates and continental crust composition. *Geochem. Cosmochim. Acta* 59, 3469–3485.
- Gaillardet, J., Dupré, B., Louvat, P., Allegre, C., 1999. Global silicate weathering and CO<sub>2</sub> consumption rates deduced from the chemistry of large rivers. *Chem. Geol.* 159, 3–30.
- Gibbs, R.J., 1970. Mechanisms controlling world water chemistry. *Science* 170, 1088–1090.
- Grosbois, C., Négrel, P., Grimaud, D., Fouillac, C., 2001. An overview of dissolved and suspended matter fluxes in the Loire River basin: natural and anthropogenic inputs. *Aquat. Geochem.* 7, 81–105.
- Han, G., Tang, Y., Xu, Z., 2010. Fluvial geochemistry of rivers draining karst terrain in

- Southwest China. *J. Asian Earth Sci.* 38, 65–75.
- Hyonjeong, N., Youngsook, H., Qin, J.H., Ellis, A., 2009. Chemical weathering in the three rivers region of eastern Tibet. *Geochem. Cosmochim. Acta* 73, 1857–1877.
- Kim, K.H., Yun, S.T., Choi, B.Y., Chae, G.T., 2009. Hydrochemical and multivariate statistical interpretations of spatial controls of nitrate concentrations in a shallow alluvial aquifer around oxbow lakes (Osong area, central Korea). *J. Contam. Hydrol.* 107, 114–127.
- Larssen, T., Seip, H.M., Semb, A., Mulder, J., Muniz, I.P., Vogt, R.D., Lydersen, E., Angell, V., Tang, D., Eilertsen, O., 1999. Acid deposition and its effects in China: an overview. *Environ. Sci. Policy* 2, 9–24.
- Li, S., Lu, X.X., Bush, R.T., 2014. Chemical weathering and CO<sub>2</sub> consumption in the lower mekong river. *Sci. Total Environ.* 472, 162–177.
- Li, Z., Coles, A.E., Xiao, J., 2019. Groundwater and streamflow sources in China's Loess Plateau on catchment scale. *Catena* 181, 075–104.
- Li, Z., Lin, X., Coles, A.E., Chen, X., 2017. Catchment-scale surface water-groundwater connectivity on China's Loess Plateau. *Catena* 152, 268–276.
- Lu, X., Li, L.Y., Lei, K., Wang, L., Zhai, Y., Zhai, M., 2010. Water quality assessment of Wei River, China using fuzzy synthetic evaluation. *Environ. Earth Sci.* 60, 1693–1699.
- Mateo-Sagasta, J., Marjani Zadeh, S., Turrall, H., 2018. More People, More Food, Worse Water? a Global Review of Water Pollution from Agriculture. FAO, Rome, Italy.
- Meybeck, M., 1998. Man and river interface: multiple impacts on water and particulates chemistry illustrated in the Seine river basin. *Hydrobiologia* 373–374, 1–20.
- Mitamura, O., Seike, Y., Kondo, K., Goto, N., Anbutsu, K., Akatsuka, T., Kihira, M., Tsering, T.Q., Nishimura, M., 2003. First investigation of ultraoligotrophic alpine Lake Puma Yumco in the pre-Himalayas, China. *Limnology* 4, 167–175.
- Moon, S., Huh, Y., Qin, J., Pho, N.V., 2007. Chemical weathering in the Hong (Red) River basin: rates of silicate weathering and their controlling factors. *Geochem. Cosmochim. Acta* 71, 1411–1430.
- Ning, T., Li, Z., Liu, W., 2017. Vegetation dynamics and climate seasonality jointly control the interannual catchment water balance in the Loess Plateau under the Budyko framework. *Hydrol. Earth Syst. Sci.* 21, 1515–1526.
- Ollivier, P., Hamelin, B., Radakovitch, O., 2010. Seasonal variations of physical and chemical erosion: a three-year survey of the Rhone River (France). *Geochem. Cosmochim. Acta* 74, 907–927.
- Phillips, D.L., Gregg, J.W., 2003. Source partitioning using stable isotopes: coping with too many sources. *Oecologia* 136, 261–269.
- Piper, A.M., 1944. A graphic procedure in the geochemical interpretation of water-analyses. *Trans. Am. Geophys. Union* 25, 914–928.
- Qu, J., Lu, S., Gao, Z., Li, W., Li, Z., Yu, F., 2017. Research on hydrogeochemical characteristics and transformation relationships between surface water and groundwater in the Weihe river. *Hydrol. Earth Syst. Sci. Discuss.* 1–14, 2017.
- Rai, S.K., Singh, S.K., Krishnaswami, S., 2010. Chemical weathering in the plain and peninsular sub-basins of the Ganga: impact on major ion chemistry and elemental fluxes. *Geochem. Cosmochim. Acta* 74, 2340–2355.
- Redwan, M., Abdel Moneim, A.A., 2016. Factors controlling groundwater hydro-geochemistry in the area west of Tahta, Sohag, Upper Egypt. *J. Afr. Earth Sci.* 118, 328–338.
- Roy, S., Gaillardet, J., Allègre, C.J., 1999. Geochemistry of dissolved and suspended loads of the Seine River, France: anthropogenic impact, carbonate and silicate weathering. *Geochem. Cosmochim. Acta* 63, 1277–1292.
- Sarin, M.M., Krishnaswami, S., Trivedi, J.R., Sharma, K.K., 1992. Major ion chemistry of the Ganga source waters: weathering in the high altitude Himalaya. *Proc. Indian Acad. Sci. Earth Planet. Sci.* 101, 89–98.
- Stallard, R.F., Edmond, J.M., 1987. Geochemistry of the amazon 3. weathering chemistry and limits to dissolved inputs. *J. Geophys. Res. Oceans* 92, 8293–8302.
- Sun, 2014. Formation Mechanism of Fluoride and Iodine in Groundwater in the Weihe River Basin and its Effect on Human Health. Changan University (in Chinese).
- Sun, H., Han, J., Li, D., Zhang, S., Lu, X., 2011. Chemical weathering inferred from riverine water chemistry in the lower Xijiang basin, South China. *Sci. Total Environ.* 408, 4749–4760.
- UNEP, 2016. A Snapshot of the World's Water Quality: towards a Global Assessment. United Nations Environment Programme, Nairobi, Kenya, p. 162.
- Villegas, P., Paredes, V., Betancur, T., Ribeiro, L., 2013. Assessing the hydrochemistry of the Urabá Aquifer, Colombia by principal component analysis. *J. Geochem. Explor.* 134, 120–129.
- Wang, L., Shen, B., Niu, S., Li, Y., Li, H., Wang, J., 2011. Analysis of Water Quality Change Trends and Causes of the Wei River, 2011 International Symposium on Water Resource and Environmental Protection, pp. 1234–1237.
- Wen, Y., Schoups, G., Nick, V.D.G., 2015. Population and Climate Pressures on Global River Water Quality. EGU General Assembly Conference Abstracts.
- Xiao, J., Zhang, F., Jin, Z.D., 2016. Spatial characteristics and controlling factors of chemical weathering of loess in the dry season in the middle Loess Plateau, China. *Hydrol. Process.* 30, 4855–4869.
- Yu, S., Xu, Z., Wu, W., Zuo, D., 2016. Effect of land use types on stream water quality under seasonal variation and topographic characteristics in the Wei River basin, China. *Ecol. Indic.* 60, 202–212.
- Zhang, B., Song, X., Zhang, Y., Han, D., Tang, C., Yu, Y., Ma, Y., 2012. Hydrochemical characteristics and water quality assessment of surface water and groundwater in Songnen plain, Northeast China. *Water Res.* 46, 2737–2748.